Millisecond Pulsars as Tools of Fundamental Physics

Michael Kramer

University of Manchester, Jodrell Bank Observatory, Cheshire SK11 9DL, UK

Abstract. A new era in fundamental physics began when pulsars were discovered in 1967. Soon it became clear that pulsars were useful tools for a wide variety of physical and astrophysical problems. Further applications became possible with the discovery of the first binary pulsar in 1974 and the discovery of millisecond pulsars in 1982. Ever since pulsars have been used as precise cosmic clocks, taking us beyond the weak-field limit of the solar-system in the study of theories of gravity. Their contribution is crucial as no test can be considered to be complete without probing the strong-field realm of gravitational physics by finding and timing pulsars. In this review, I will explain some of the most important applications of millisecond pulsar clocks in the study of gravity and fundamental constants.

1 Introduction

The title of this volume, "Astrophysics, Clocks, and Fundamental Constants", would also be a suitable title for this contribution describing the use of radio pulsars in the study of fundamental physics. Indeed, pulsar astronomy is an extraordinary discipline which removes the distinction between physics and astrophysics that is often made. Such a distinction may be justified by the fact that in a terrestrial laboratory we can modify the experimental set-up and control the environment. In contrast, in astrophysical experiments we remain an observer, deriving all our information simply from observing photons and their properties. Thereby, terrestrial experiments are typically more precise and, most importantly, can be reproduced – at least in principle – in any other laboratory on Earth. However, when probing the limits of our understanding of fundamental physics, we often have to study conditions that are too extreme to be encountered on Earth. One may take the experiment into space, like "LISA", "STEP" or "Gravity Probe-B", but even then we are limited, particularly if we want to study gravity. While solar system tests provide a number of very stringent tests for general relativity, none of the experiments made or proposed for the future will ever be able to test the strong field limit. For such studies, pulsars are and will remain the only way to test and enhance our understanding. Additionally, pulsars not only provide us with the only means to perform strong-field experiments, but these experiments are also amazingly precise. It is this unique aspect that I will review in the following. The interested reader may also consult the excellent reviews by Will [40] and Turyshev (this volume) on PPN formalism, by Wex [37] and Stairs [30] on strong gravity tests, and by Lorimer [22] on pulsars in general.

2   Pulsars

Pulsars are highly magnetized, rotating neutron stars which emit a narrow radio beam along the magnetic dipole axis. As the magnetic axis is inclined to the rotation axis, the pulsar acts like a cosmic light-house emitting a radio pulse that can be detected once per rotation period when the beam is directed towards Earth (Figure 1). For some very fast rotating pulsars, the so-called millisecond pulsars, the stability of the pulse period is similar to that achieved by the best terrestrial atomic clocks. This is not surprising if we consider that they have large rotational energies of $E = 10^{43-45}$ J and low energy loss rates. Using these astrophysical clocks by accurately measuring the arrival times of their pulses, a wide range of experiments is possible, some of which are presented here. While it is not of utmost importance for the remainder of this review *how* the radio pulses are actually created, we will consider some of the basic pulsar properties below.

2.1   Pulsars as Neutron Stars

Pulsars are born in supernova explosions of massive stars. Created in the collapse of the stars' core, neutron stars are the most compact objects next to black holes. From timing measurements of binary pulsars (see Section 5.2), we determine the masses of pulsars to be within a narrow range of $1.35 \pm 0.04 M_\odot$[34]. Modern calculations for different equations of state produce results for the size of a neutron star quite similar to the very first calculations by Oppenheimer & Volkov [27], i.e. about 20 km in diameter. Such sizes are consistent with independent estimates derived from modelling light-curves and luminosities of pulsars observed in X-rays (e.g. [42]).

As rotating magnets, pulsars emit magnetic dipole radiation as the dominant effect for an increase in rotation period, P, described by $\dot{P}$. Equating the corresponding energy output of the dipole to the loss rate in rotational energy, we obtain an estimate for the magnetic field strength at the pulsar surface

$$B_S = 3.2 \times 10^{19} \sqrt{P\dot{P}} \text{ Gauss} \tag{1}$$

Sometimes twice the value is quoted to reflect the field at the poles. Typical values are of order 10^{12} G, although field strengths up to 10^{14} have been observed [25]. Millisecond pulsars have lower field strengths of the order of 10^8 to 10^{10} Gauss which appear to be a result of their evolutionary history (see Section 3). These magnetic fields are consistent with values derived from X-ray spectra of neutron stars where we observe cyclotron lines [7].

2.2   Pulsars as Radio Sources

The radio signal of a pulsar is usually weak, both because the pulsar is distant and the size of the actual emission region is small. Estimates range down to a few metres, resulting in brightness temperatures of up to 10^{37} K [14]. Such values
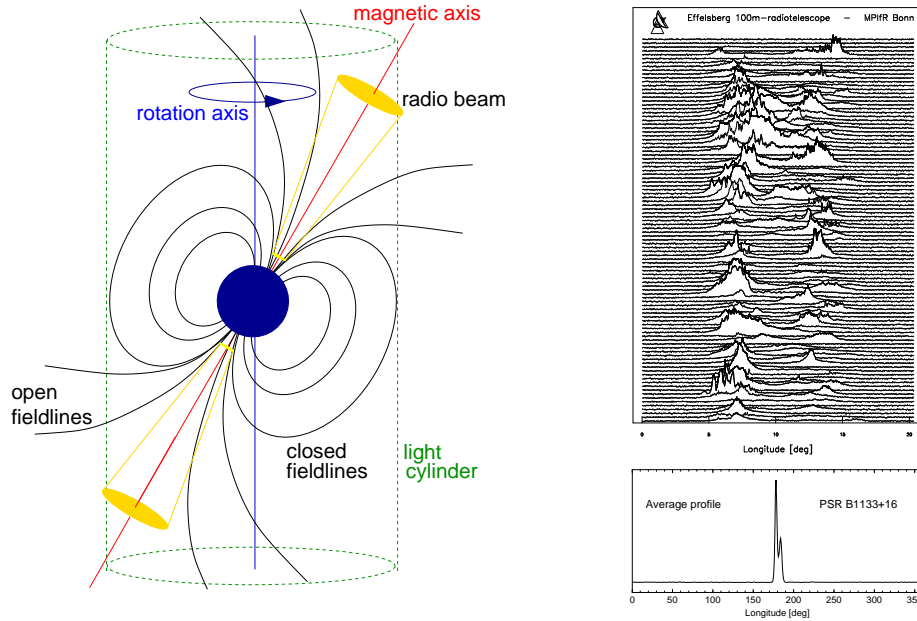
Fig. 1. left) A pulsar is a rotating, highly magnetised neutron star. A radio beam centred on the magnetic axis is created at some height above the surface. The tilt between the rotation and magnetic axes makes the pulsar in effect a cosmic lighthouse when the beam sweeps around in space right) Individual pulses vary in shapes and strength (top) average profiles are stable (bottom). The typical pulse width is only ~4% of the period.

require a coherent emission mechanism which, despite 35 years of intensive research, is still unidentified. However, we seem to have some basic understanding, in which the magnetized rotating neutron star induces an electric quadrupole field which is strong enough to pull out charges from the stellar surface (the electrical force exceeds the gravitational force by a factor of $\sim 10^{12}$!). The magnetic field forces the resulting dense plasma to co-rotate with the pulsar. This *magnetosphere* can only extend up to a distance where the co-rotation velocity reaches the speed of light[1]. This distance defines the so-called light cylinder which separates the magnetic field lines into two distinct groups, i.e. *open and closed field lines*. The plasma on the closed field lines is trapped and co-rotates with the pulsar forever. In contrast, plasma on the open field lines can reach highly relativistic velocities and can leave the magnetosphere, creating the observed radio beam at a distance of a few tens to hundreds of km above the pulsar surface (e.g. [17], see Fig. 1).

---

[1] Strictly speaking, the Alfvén velocity will determine the co-rotational properties of the magnetosphere.

Most pulsars are not strong enough for us to allow studies of their individual radio pulses. Then, only an integrated pulse shape, the "pulse profile", can be observed. Individual pulses reflect the instantaneous plasma processes in the pulsar magnetosphere, resulting in often seemingly random pulses (see Fig. 1). In contrast, the average pulse profile reflects the global constraints mostly given by a conal beam structure and geometrical factors and is thereby stable. It is this profile stability which allows us to time pulsar to high precision.
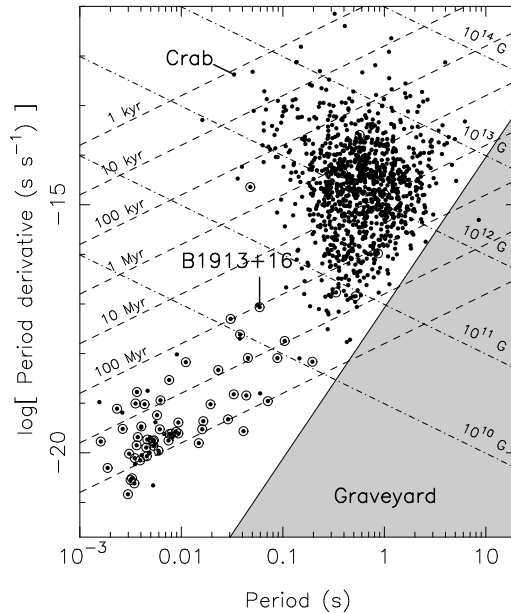

Fig. 2. The $P - \dot{P}$–diagram for the known pulsar population. Lines of constant characteristic age and surface magnetic field are shown. Binary pulsars are marked by a circle. The solid line represents the pulsar "death line" enclosing the "pulsar graveyard" where pulsars are expected to switch off radio emission.

3   A Pulsar's Life

The evolution in pulsar period, P, and slow-down, $\dot{P}$, can be used to describe the life of a pulsar. This is usually done in a (logarithmic) P-$\dot{P}$-diagram as shown in Figure 2 where we can draw lines of constant magnetic field (see Eqn. 1) and constant "characteristic age" estimated from

$$\tau = \frac{P}{2\dot{P}} = -\frac{\nu}{2\dot{\nu}} \tag{2}$$

using either period, P, or the spin frequency, ν, and their derivatives. This quantity is a valid estimate for the true age under the assumption that the

initial spin period is much smaller than the present period and that the spin-down is fully determined by magnetic dipole braking. While it had been assumed that pulsars are born with birth periods similar to that estimated for the Crab pulsar, $P_0 = 19$ ms [23], recent estimates for a growing number of pulsars suggest a wide range of initial spin periods from 14 ms up to 140 ms [20]. Pulsars are therefore born in the upper left area of Fig. 2 and move into the central part where they spent most of their lifetime.

3.1   Normal Pulsars

Most known pulsars have spin periods between 0.1 and 1.0 sec with period derivatives of typically $\dot{P} = 10^{-15}$ s s^{-1}. Selection effects are only partly responsible for the limited number of pulsars known with very long periods, the longest known period being 8.5 s [41]. The dominant effect is due to the "death" of pulsars when their slow-down has reached a critical state. This state seems to depend on a combination of P and $\dot{P}$ which can be represented in the $P - \dot{P}$-diagram as a "pulsar death-line". To the right and below this line (see Figure 2) the electric potential above the polar cap may not be sufficient to produce the particle plasma that is responsible for the observed radio emission. While this model can indeed explain the lack of pulsars beyond the death-line, the truth may be more complicated as the position of the 8.5-sec pulsar deep in the "pulsar graveyard" indicates. Nevertheless, it is clear that the normal life of radio pulsars is limited and that they die eventually after tens to a hundred million years.

3.2   Millisecond Pulsars

Inspecting the approx. 1600 sources shown in the $P - \dot{P}$-diagram, it is obvious that the position of a sub-set of about 100 pulsars located in the lower left part of the diagram cannot be explained by the above picture of normal pulsar life. Instead, these pulsars simultaneously have small periods (of the order of milliseconds) and small period derivatives, $\dot{P} \lesssim 10^{-18}$ s s^{-1}. They appear much older than ordinary pulsars (see Eqn. 2) and, indeed, these so-called "millisecond pulsars" represent the oldest population of pulsars with ages up to $\sim 10^{10}$ yr. A model for their evolutionary history was proposed soon after the discovery of PSR B1937+21 by Backer et al. in 1982[4]. This first millisecond pulsar has a period of only 1.56 ms and remains the pulsar with the shortest period known.

It is suggested that millisecond periods are obtained when mass and thereby angular momentum is transferred from an evolving binary companion while it overflows its Roche lobe [1]. In this model, millisecond pulsars are recycled from a dead binary pulsar via an X-ray binary phase. This model implies a number of observational consequences: a) most normal pulsars do not develop into a millisecond pulsar as they have long lost a possible companion during their violent birth event; b) for surviving binary systems, X-ray binary pulsars represent the progenitor systems for millisecond pulsars; c) the final spin period of recycled pulsars depends on the mass of the binary companion. A more massive companion evolves faster, limiting the duration of the accretion process; d) the

majority of millisecond pulsars have low-mass white-dwarf companions as the remnant of the binary star. These systems evolve from low-mass X-ray binary systems (LMXBs); e) high-mass X-ray binary systems (HMXBs) represent the progenitors for double neutron star systems (DNSs). DNSs are rare since these systems need to survive a second supernova explosion. The resulting millisecond pulsar is only mildly recycled with a period of tens of millisecond.

The properties of millisecond pulsars and X-ray binaries are consistent with the described picture. For instance, it is striking that $\sim 90\%$ of all millisecond pulsars are in a binary orbit while this is true for only less than 1% of the non-recycled population. For millisecond pulsars with a low-mass white dwarf companion the orbit is nearly circular. In case of double neutron star systems, the orbit is affected by the unpredictable nature of the kick imparted onto the newly born neutron star in the asymmetric supernova explosion of the companion. If the system survives, the result is typically an eccentric orbit with an orbital period of a few hours. As we will see, both types of system can be used to test different aspects of gravitational theories.

4   Pulsars as Clocks

By measuring the arrival time of the received ticks of the pulsar clock very precisely, we can study effects that determine the propagation of the pulses in four-dimensional space-time. Millisecond pulsars are the most useful objects for these investigations: their pulse arrival times can be measured much more accurately than for normal pulsars (the measurement precision scales essentially with spin frequency) and their rotation is much smoother, making them intrinsically better clocks. Specifically, they do not exhibit rotational instabilities known for normal pulsars, namely "timing noise" and "glitches". Glitches are associated with young pulsars and they represent a sudden increase in rotation frequency that is probably caused by an abrupt change in the internal structure of the neutron star. The origin of timing noise is much less understood. It manifests itself in a quasi-random walk in one or more of the rotational parameters on timescales of months to years. Again, it appears mostly for young pulsars and scales with some power of the period derivative, $\dot{P}$. Hence, millisecond pulsars generally do not show timing noise, although it has been detected for few sources such as PSR B1937+21 [16] albeit on a much smaller amplitude scale than for normal pulsars.

4.1   Time Transfer

In order to study effects that change the pulse travel time, we first have to find an expression that describes the pulsar rotation in a reference frame co-moving with the pulsar. We start by expressing the spin frequency of the pulsar in a Taylor expansion,

$$\nu(t) = \nu_0 + \dot{\nu}(t - t_0) + \frac{1}{2}\ddot{\nu}(t - t_0)^2 + \dots \tag{3}$$

where ν_0 is the spin frequency at reference time t_0, i.e. $\nu_0 = \nu(t_0) = 1/P_0$ with P_0 being the corresponding pulse period. While ν_0 is referring to a certain epoch, the parameters $\dot{\nu}$, $\ddot{\nu}$ are determined by the physical process responsible for the pulsar slow-down and should be constant for most time-spans considered.[2] We expect a relation of

$$\dot{\nu} = -\text{const.}\, \nu^n \qquad (4)$$

and hence $\ddot{\nu} = -\text{const.}\, n\ \nu^2\ \dot{\nu}$ where the "braking index", n, has a value of $n = 3$ for magnetic dipole braking, relating to Eqn. 2. Measuring $\ddot{\nu}$ can yield the braking index via $n = \nu\ddot{\nu}/\dot{\nu}^2$ so that the assumption of dipole braking can be tested. Timing noise can mimic a significant but time-varying value of $\ddot{\nu}$ that reflects timing noise rather than regular spin-down. In these cases, derived braking indices are meaningless. For almost all millisecond pulsars $\ddot{\nu}$ is too small to be of significance.

Relating the spin frequency to the pulse number N, $\nu = dN/dt$, we find

$$N = N_0 + \nu_0(t - \tau_0) + \frac{1}{2}\dot{\nu}(t - t_0)^2 + \frac{1}{6}\ddot{\nu}(t - t_0)^3 + ... \qquad (5)$$

where N_0 is the pulse number at the reference epoch t_0. If the pulsar spin-down is accurately known, the pulses should therefore appear at integer values of N when observed in an inertial frame of the pulsar.

Our observing frame unfortunately is not inertial, as we are using telescopes that are located on a rotating Earth orbiting the Sun. Before analysing corresponding TOAs measured with the observatory clock ("topocentric arrival times"), we need to transfer them to the centre of mass of the solar system as the best approximation to an inertial frame available. By using such "barycentric arrival times", we can easily combine transferred topocentric TOAs measured at different observatories at different times. The transformation of a topocentric TOA to a barycentric arrival time, t_{SSB}, is given by

$$t_{\text{SSB}} = \quad t_{\text{topo}} - t_0 + t_{\text{corr}} - D/f^2 \ , \qquad (6a)$$
$$+ \ \Delta_{\text{Roemer},\odot} + \Delta_{\text{Shapiro},\odot} + \Delta_{\text{Einstein},\odot} \ , \qquad (6b)$$
$$+ \ \Delta_{\text{Roemer,Bin}} + \Delta_{\text{Shapiro,Bin}} + \Delta_{\text{Einstein,Bin}} \qquad (6c)$$

We have split the transformation into three lines. The first two lines apply to every pulsar whilst the third line is only applicable to binary pulsars. We discuss each term in detail.

Clock and frequency corrections The observatory time is typically maintained by local H-maser clocks that are compared to UTC(NIST) by the Global Positioning System (GPS). Offsets are monitored and retroactively applied as clock corrections, t_{corr}, in the off-line analysis which finally uses UTC of BIPM as time standard, in general. Further corrections take into account that the Earth is not rotating uniformly, modifying the effective arrival time at the telescope.

---

[2] Hence we do not add a subscript to these parameters.

Such UT1 corrections utilize Earth rotation data published by the International Earth Rotation Service (IERS). Moreover, leap seconds, that are introduced into UTC to keep it close mean solar time, are now removed from the used UTC time standard to produce a TOA measured in Terrestrial Dynamic Time, TDT, which is also called TAI (International Atomic Time).

As the pulses are delayed due to dispersion in the interstellar medium, the arrival time depends on the observing frequency, f. The TOA is therefore corrected for a pulse arrival at an infinitely high frequency, thereby removing dispersion from the data (last term in Eqn. 6a). The corresponding Dispersion Measure is determined during the discovery of the pulsar and can be improved in its accuracy by performing multi-frequency timing observations.

Barycentric corrections The terms in Eqn. 6b describe the corrections necessary to transfer topocentric to barycentric TOAs.

The *Roemer delay*, $\Delta_{\mathrm{Roemer},\odot}$, corrects for (classical) light-travel time from the telescope to the Solar System Barycentre (SSB) and can be be computed from the dot product of a unit vector, $\hat{s}$, pointing from the SSB to the position of the pulsar, and the vector pointing from the observatory to the SSB, r, which can be separated into three parts,

$$\Delta_{\mathrm{Roemer},\odot} = \frac{1}{c}\, r \cdot \hat{s} = \frac{1}{c}\,(r_{\mathrm{OE}} + r_{\mathrm{ES}} + r_{\mathrm{SSB}}) \cdot \hat{s} \qquad (7)$$

The first vector, r_{OE}, connects the phase centre of the observing telescope with the centre of the Earth, the second vector, r_{ES}, spans from the geocentre to the centre of the Sun, whilst the last contribution, r_{SSB}, takes into account that the SSB is actually outside the Sun's "surface" due to the presence of Jupiter. These corrections obviously require accurate knowledge of the locations of all major bodies in the Solar system. This is achieved by using solar system ephemerides such as the "DE200" or "DE405" published by JPL [32].

The *Shapiro delay*, $\Delta_{\mathrm{Shapiro},\odot}$, is a relativistic correction that corrects for an extra delay due to the curvature of space-time in the solar system [29]. It is largest for a signal passing the Sun's limb ($\sim 120\ \mu$s) while Jupiter can contribute as much as 200 ns. In principle one has to sum over all bodies in the solar system, yielding

$$\Delta_{\mathrm{Shapiro},\odot} = (1 + \hat{\gamma}) \sum_i \frac{GM_i}{c^3} \ln \left[\frac{\hat{s}_i\, r_i^E + r_i^E}{\hat{s}_i\, r_i^P + r_i^P} \right] \qquad (8)$$

where M_i is the mass of body i, r_i^P is the pulsar position relative to it, and r^E the position relative to that body at the time of closest approach of the [3]). The parameter $\hat{\gamma}$ is one of the Parameterized-Post-Newtonian meters that will be discussed in Section 5.1. It describes how much ture is produced by unit rest mass and takes the value $\hat{\gamma} = 1$ in tivity. [3] In practice, only the Sun is taken into account in the sum,

---

[3] Usually, this parameter is denoted without the "hat" simply as γ (see contribution by Turyshev), but it is common practice in the study of binary pulsars to use the symbol γ to describe the amount of gravitational redshift caused by the pulsar companion.

but if a pulsar-Jupiter ocultation occurs during the experiment, it may need to be included.

The last term in Eqn. 6b, $\Delta_{\mathrm{Einstein},\odot}$, is called *Einstein delay* and it describes the combined effect of gravitational redshift and time dilation due to motion of the Earth and other bodies, taking into account the variation of an atomic clock on Earth in the varying gravitational potential as it follows its elliptical orbit around the Sun [3]. The delay amounts to an integral of the expression

$$\frac{d\Delta_{\mathrm{E}instein,\odot}}{dt} = \sum_i \frac{GM_i}{c^2 r_i^E} + \frac{v_E^2}{2c^2} - \mathrm{constant} \tag{9}$$

where the sum is again over all bodies in the solar system but this time excluding Earth. The distance r_i^E is again the distance between Earth and body i, while v_E is the velocity of the Earth relative to the Sun.

By introducing the Einstein delay into Eqn. 6b, we transfer TDT into a uniformly running coordinate time at the SSB and, hence, Barycentric Dynamical Time (TDB). One could hide the explicit appearance of $\Delta_{\mathrm{E}instein,\odot}$ if we adopted TDB as our formal time standard rather than starting off with our observatory clock corrected to TDT. However, since the same effects that cause the Einstein delay in the solar system also affect the pulsar clock in a binary orbit around a companion, it is useful to write $\Delta_{\mathrm{E}instein,\odot}$ explicitly alongside with a similar term for binary pulsars, $\Delta_{\mathrm{E}instein,Bin}$. It appears in Eqn. 6c with similar terms describing Roemer and Shapiro delay in the binary orbit.

Relative Motion Equation 6a-6c is sufficient to measure the clock rate as produced by the pulsar if no further motion or acceleration between pulsar and SSB occurs. If the pulsar is moving relative to the SSB, only the transverse component of the velocity, v_t, can be observed. A radial motion is not measurable, unless the pulsar has an optically detectable companion such as a white dwarf for which Doppler shifts can be measured from optical spectra. Otherwise, the effects of any radial velocity are absorbed in Doppler corrections to the observed periods and cannot be determined. In contrast, the transverse motion will change the vector $\hat{s}$ in Eqn. 7, adding a linear time-dependent term to our transfer equation, and can therefore be measured as proper motion, μ.

Another effect arising from a transverse motion is the *Shlovskii* (1970) *effect*, also known in classical astronomy as "secular acceleration". With the pulsar motion, the projected distance of the pulsar to the SSB is increasing, leading to a correction that is quadratic in time [3],

$$\Delta t_S = \frac{v_t^2}{2dc}\, t^2. \tag{10}$$

Since this delay scales with inverse of the distance d to the pulsar, the correction is usually too small to be considered. However, it has the effect that any observed change in a periodicity (i.e. change in pulse or orbital period) is increased over the intrinsic value by

$$\frac{\dot{P}}{P} = \frac{1}{c}\frac{v_t^2}{d} = \frac{d}{c}\mu^2 \tag{11}$$

For millisecond pulsars where $\dot{P}$ is small, a significant fraction of the observed change in period can be due to the Shlovskii effect. This effect also needs to be considered, when studying the decay of an orbital period due to gravitational wave emission, where the observed value is increased by the Shlovskii term. Similarly, any acceleration of the pulsar due to an external gravitational field, e.g. if the pulsar is located in a globular cluster, also modifies period derivatives by an amount $\dot{P}/P = a/c$ where a is the acceleration [28].

Finally, a related term that needs to be considered for nearby pulsars describes an annual parallax given by [3]

$$\Delta t_\pi = -\frac{1}{2cd}\left(\boldsymbol{r}\times\hat{\boldsymbol{s}}\right) = \frac{1}{2cd}\left((\boldsymbol{r}\cdot\hat{\boldsymbol{s}})^2 - |\boldsymbol{r}|^2\right) \tag{12}$$

In comparison to the more familiar positional parallax, this *timing parallax* corresponds to measuring the time delay due to the curvature of the emitted wavefronts at different positions of the Earth orbit. This effect imposes a signal with an amplitude of $l^2\cos\beta/(2cd)$ where l is the Earth-Sun distance and β is the ecliptic latitude of the pulsar. For a pulsar at $d = 1$ kpc, this delay amounts to only $\lesssim 1.2\mu$s, and hence it is only measurable for a few millisecond pulsars where it provides a precise distance estimate. Similarly difficult to measure is the *annual-orbital parallax* for binary pulsars which manifests itself as a periodic change in the observed projected semi-major axis of the pulsar's orbit due to viewing the system from slightly different directions during the Earth's orbit. In contrast, a secular change of the semi-major axis due to a proper motion of the system on the sky has been measured for a number of binary millisecond pulsars (see [30]).

4.2   Pulsar Timing

The transfer equation Eqn. 6a-6c contains a number of parameters which are not known *a priori* (or only with limited precision after the discovery of a pulsar) and need to be determined precisely in a least-squares fit analysis of the measured TOAs. These parameters can be categorised into three groups:

Astrometric parameters: The astrometric parameters include the position of the pulsar, and its proper motion and parallax. While the position is only known within a telescope beam after the discovery, the precision can be greatly improved by timing the pulsar for about a year (full Earth orbit). Proper motion and parallax only become evident after a longer time-span.

Spin parameters: These include the rotation frequency of the pulsar, ν, and its derivatives (Eqn. 3).

Binary parameters: For pulsars in a binary orbit, the initial observations will typically show a periodic variation in observed pulse period. Five Keplerian parameters then need to be determined: orbital period, P_b; the projected semi-major axis of the orbit, $x \equiv a\sin i$ where i is the (usually unknown) inclination angle of the orbit; the orbital eccentricity, e; the longitude of
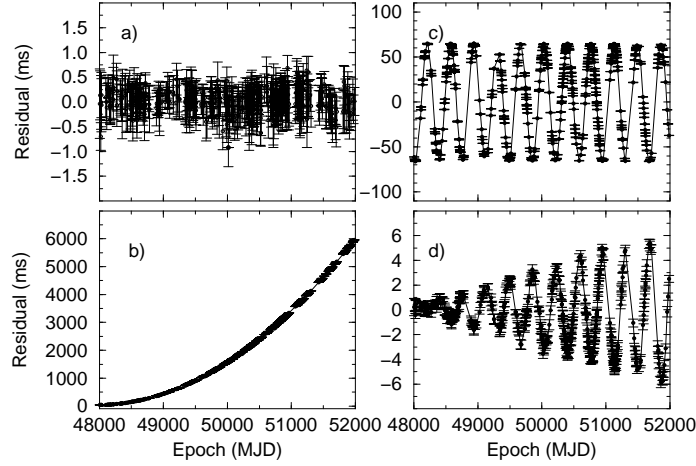
Fig. 3. Timing residuals for the 1.19-s pulsar B1133+16. A fit of a perfect timing model should result in randomly distributed residuals, shown in a). A parabolic increase in the residuals in part b) is obtained if $\dot{P}$ is underestimated, here by 4%. An offset in position produces sinusoid residuals shown in part c) where the declination has an error of 1 arcmin. Part d) demonstrates the effect of neglected proper motion, here of $\mu = 380$ mas/yr. Note the different scales on the y-axes.

periastron, ω; and the time of periastron passage, T_0. For a number of binary systems this Newtonian description of the orbit is not sufficient and relativistic corrections need to be applied, e.g. ω is replaced by $\omega + \dot{\omega}t$. The measurement of the *Post-Keplerian* (PK) *parameters* such as $\dot{\omega}$ allows a comparison with values expected in the framework of specific theories of gravity. We discuss these aspects further below.

Given a minimal set of starting parameters, a least-squares fit is needed to match the measured arrival times to pulse numbers according to Eqn. 5. The aim is to obtain a phase-coherent solution that accounts for every single rotation of the pulsar between two observations. One starts off with a small set of TOAs that were obtained so closely in time, that the accumulated uncertainties in the starting parameters do not exceed one pulse period. Gradually, the data set is expanded, maintaining coherence in phase. When successful, post-fit residuals expressed in pulse phase show a random distribution around zero (see Fig 3). After starting with fits for only period and pulse reference phase over some hours and days, longer time spans slowly require fits for parameters like spin-frequency derivative(s) and position. Incorrect or incomplete timing models cause systematic structures in the post-fit residuals identifying the parameter that needs to be included or adjusted (see Fig. 3). The precision of the parameters improves with length of the data span and the frequency of observation, but also with orbital coverage in the case of binary pulsars. Sufficient data sets then enable measurements with amazing precision, e.g. the period determined for PSR B1937+21 is known to a relative precision of 10^{-16}.

Obviously, the above description shows that the process of pulsar timing is elaborate. Fortunately, sophisticated software packages have been developed that combine time transfer and the least-squares fit of the timing model. The three major packages are TEMPO (ATNF/Princeton University)[4], PSRTIME (Jodrell Bank Observatory)[5] and TIMAPR (Pushchino Observatory/MPIfR)[6]. The most widely used package is TEMPO.

5   Applications of Pulsars

Pulsars are unique and versatile objects which can be used to study an extremely wide range of physical and astrophysical problems. Beside testing theories of gravity one can study the Galaxy and the interstellar medium, stars, binary systems and their evolution, solid state physics and the interior of neutron stars. Investigating the radio emission of pulsars provides insight into plasma physics under extreme conditions. In the following we will concentrate on the application of pulsars as clocks, paying in particular attention to tests of theories of gravity. Some of these tests involve studies of *PPN parameters* and possible related time variation in the Gravitational Constant, G.

5.1   PPN parameters

Metric theories of gravity assume *(i)* the existence of a symmetric metric, *(ii)* that all test bodies follow geodesics of the metric and *(iii)* that in local Lorentz frames the non-gravitational laws of physics are those of special relativity. Under these conditions we can study metric theories with the *Parameterized Post-Newtonian* (PPN) formalism by describing deviations from simple Newtonian physics in the slow-motion and weak-field limit. This is possible in a theory-independent fashion, such that the only differences in these theories occur in the numerical coefficients that appear in the metric, characterised by a set of 10 real-valued PPN-Parameters [26]. Each of the parameters can be associated with a specific physical effect, like the violation of conversation of momentum or equivalence principles, and certain values are assigned to them in a given theory. Thereby, comparing measured PPN parameters to their theoretical values can single out wrong theories in a purely experimental way. A more complete description of the PPN formalism and the physical meaning of PPN parameters is presented by Turyshev in this volume. A recent review was given by Will [40]. Here we summarize the studies of those PPN parameters that can be constrained by pulsars. A more detailed account of related pulsar tests is given by Wex [36,37] and Stairs [30].

---

[4] http://pulsar.princeton.edu/tempo/

[5] http://www.jb.man.ac.uk/research/pulsar/observing/progs/progs.html

[6] http://www.mpifr-bonn.mpg.de/div/pulsar/former/olegd/soft.html

Violations of the Strong-Equivalence-Principle (SEP) The *Strong Equivalence Principle* (SEP) is completely embodied into general relativity, while alternative theories of gravity predict a violation of some or all aspects of SEP. The SEP is, according to its name, stronger than both the *Weak Equivalence Principle* (WEP) and the *Einstein Equivalence Principle* (EEP). The WEP states that all test bodies in an external gravitational field experience the same acceleration regardless of the mass and composition. While the WEP is included in all metric theories of gravity, the EEP goes one step further and also postulates *Lorentz-invariance* and positional invariance. Lorentz-invariance means that no preferred frame exists, so the outcome of a local non-gravitational experiment is independent from the velocity of the apparatus, while positional invariance renders it unimportant where this experiment is being performed. The SEP includes both the WEP and the EEP, but postulates them also for gravitational experiments. As a consequence, both Lorentz- and positional invariance should be independent of the gravitational self-energy of the bodies in the experiment. Obviously, all bodies involved in terrestrial lab experiments possess only a negligible fraction of gravitational self-energy, so that tests of SEP require the involvement of astronomical objects.

A violation of SEP means that there is a difference between gravitational mass, M_g, and inertial mass, M_i. The difference can be written as

$$\frac{M_g}{M_i} \equiv 1 + \delta(\epsilon) = 1 + \eta\epsilon + \mathcal{O}(\epsilon^2) \tag{13}$$

where ϵ is the gravitation self-energy in units of mc^2 and η is a parameter characterising the violation of SEP. The latter parameter was introduced by Nordvedt (1968) who suggested studying the Earth-Moon system to test for violations of SEP. Due to their different self-energy (Earth: $\epsilon \sim -4.6 \times 10^{-10}$, Moon: $\epsilon \sim -0.2 \times 10^{-10}$), Earth and Moon would fall differently in the external gravitational field of the Sun, leading to a polarization of the Earth-Moon orbit ("Nordvedt-effect"). Lunar-laser-ranging experiments can be used to put tight limits on η which is a linear combination of PPN parameters representing effects due to preferred locations, preferred frames and the violation of the conversation of momentum. However, even in the Earth-Moon case, or the Solar system in general, the self-energies involved are still small and do not test the SEP in strong-field regimes where deviations to higher order terms of ϵ could be present. It is at that point where the circular pulsar-white dwarf systems become important.

For neutron stars, $\epsilon \sim 0.15$, which is large, in particular considering $\epsilon = 0.5$ for a black hole, and much larger than the self-energy of a white dwarf, $\epsilon \sim 10^{-4}$. Therefore, the pulsar and white dwarf companion of a binary system should feel a different acceleration due to the external Galactic gravitational field if SEP is violated. Similar to the Nordvedt effect, this should lead to a polarisation of the pulsar-white dwarf orbit ("gravitational Stark effect" [12]). The eccentricity vector of such a binary system should therefore have two components, one constant component due to the external acceleration, and another one that evolves

in time following relativistic periastron advance. Since the present direction of the evolving eccentricity vector is unknown, a careful analysis of all relevant systems in a statistical manner is needed. Significant contributions to the results are made by long orbital-period and small-eccentricity systems, i.e. where P_b/e^2 is large [36].

Preferred-Frames & Conversation Laws Some metric theories of gravity violate SEP specifically by predicting preferred-frame and preferred-location effects. A preferred universal rest frame, presumably equivalent with that of the Cosmic Microwave Background (CMB), may exist if gravity is mediated (in part) by a long-range vector field. This violation of local Lorentz-invariance is described by the two PPN parameters α_1 and α_2. While both parameters can be tightly constrained in the weak-field limit of the solar system, α_1 can also be studied in the strong-field regime by analysing the same low-eccentricity pulsar-white dwarf systems with a figure-of-merit given by $P_b^{1/3}/e$: If α_1 were different from zero, a binary system moving with respect to a preferred universal rest frame would again suffer a long-term change in its orbital eccentricity. In a statistical analysis similar to that for the study of the gravitational Stark-effect, the binary 5.3-ms pulsar PSR J1012+5307 is particularly valuable. It not only has the smallest known eccentricity, for which only an upper limit of $e < 8 \times 10^{-7}$ (68% C.L.) was found from Jodrell Bank and Effelsberg observations [21], but its optically detected white dwarf companion also provides full 3-d velocity information relative to the CMB. Using this and other systems, Wex [36,37] derives $|\alpha_1| < 1.2 \times 10^{-4}$ (95% C.L.) which is slightly better than the solar system limit (see Turyshev, this volume).

In cases where theories both violate the Lorentz-invariance and the conversation of momentum, the equation of motion for a rotating body in the post-Newtonian limit contains so-called self-acceleration terms. This self-acceleration of the body's centre depends on the internal structure of the rotating body and results from the breakdown in conversation of total momentum. Another term in the self-acceleration involves the body's motion relative to a universal rest frame. Both contributions relate to the PPN parameter α_3 that can be tested using pulsars as isolated rotating objects [39,6], or as bodies in binary systems where both pulsar and companion suffer self-acceleration, leading to polarized orbits [5]. The limits derived by this second method using circular pulsar-white dwarf systems are much tighter than studying the spin periods of isolated pulsars, resulting in $|\alpha_3| < 1.5 \times 10^{-19}$ (95% C.L.) [6]. This result for α_3 and a limit set on $(\alpha_3 + \zeta_2) < 4 \times 10^{-5}$ [38] constrains the PPN parameter ζ_2, which describes the non-conversation of momentum. Derived from a limit on the second period derivative, $\ddot{P}$, of PSR B1913+16 and, hence, its acceleration, the interpretation of this limit may be complicated as non-zero $\ddot{P}$s could arise from a number of sources such as timing noise [30].

Gravitational Dipole Radiation Essentially any metric theory of gravity that embodies Lorentz-invariance in its field equations predicts gravitational ra-

diation. However, the details of these predictions may differ in the speed of the gravity waves, the polarization of the waves and/or the multi-polarities of the radiation. If a theory satisfies SEP, like general relativity, gravitational dipole radiation is not expected, and the quadrupole emission should be the lowest multipole term. This arises because the dipole moment (centre of mass) of isolated systems is uniform in time due to the conservation of momentum and because the inertial mass that determines the dipole moment is the same as the mass that generates gravitational waves. In alternative theories, while the *inertial* dipole moment may remain uniform, the *gravity wave* dipole moment may not, since in a violation of SEP the mass generating gravitational waves depends differently on the internal gravitational binding energy of each body than does the inertial mass [40]. If dipole radiation is predicted, the magnitude of this effect depends on the difference in gravitational binding energies, expressed by the difference in coupling constants to a scalar gravitational field, $(\hat{\alpha}_p - \hat{\alpha}_c)$. For a white dwarf companion $|\alpha_c| \ll |\alpha_p|$, so that the strongest emission should occur for short-orbital period pulsar-white dwarf systems. Again, the binary pulsar J1012+5307 becomes extremely useful. Given its vanishing eccentricity, the change in orbital period due to dipole radiation becomes

$$\dot{P}_b^{\mathrm{dipole}} \simeq \frac{4\pi^2 G_*}{c^3 P_b} \frac{M_p M_c}{M_p + M_c} \hat{\alpha}_p{}^2 + \mathcal{O}\left(\frac{v^5}{c^5}\right) \tag{14}$$

where G_* is the "bare" gravitational constant. With the optically detected companion, the measured radial velocity can be use to correct for Doppler effects. For this system [21], Wex [37] derives a limit of $|\hat{\alpha}_p|^2 < 4 \times 10^{-4}$ (95% C.L.).

Time Variability of the Gravitational Constant Three different pulsar tests are available to test the time variability of the gravitational constant, G, and to derive an upper limit for $\dot{G}/G$. A time variability is only allowed if SEP is violated due to preferred locations in space and time. In the case of pulsars, a changing G would change the gravitational binding energy of a neutron star and thereby possibly also its moment of inertia, which would cause a change in the spin-down behaviour, namely a contribution to $\dot{P}$. A comparison with observed values leads to limits of the order of $\dot{G}/G < 10^{-11}$ yr^{-1} [30]. A slightly more stringent limit can be derived from the effects that a varying G would have on orbital periods [13,2]. Both limits are still about an order of magnitude above the limits set by solar system tests. Moreover, they depend to some degree on the compactness of the neutron star and its equation of state, so that they are not truly theory independent [40]. An interesting alternative test uses the mass determination for neutron stars [33], utilising that the Chandrasekhar mass depends directly on G. Studying the mass of millisecond pulsars as function of pulsar age, a strong limit of $\dot{G}/G < (-0.6 \pm 4.2) 10^{-12}$ yr^{-1} (95% C.L.) is derived. However, while the mass of neutron stars can be determined quite accurately in relativistic binaries (see Section 5.2), an age estimation relying on Eqn. 2 can contain considerable uncertainty.
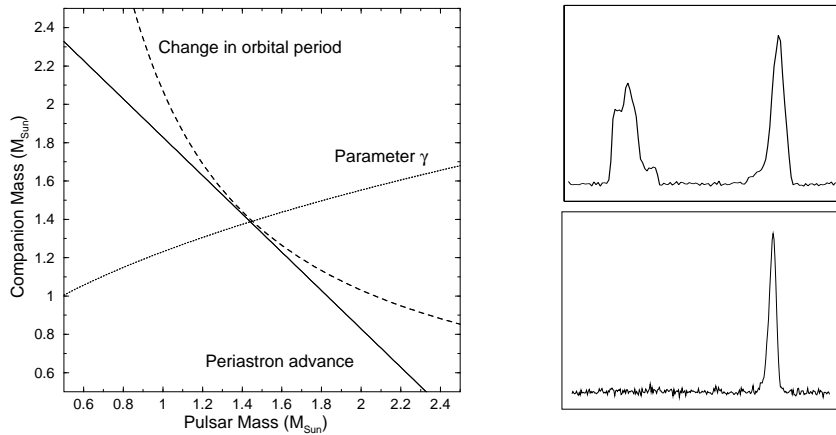
Fig. 4. left) Mass-mass diagram for the DNS PSR B1913+16 using parameters determined by Weisberg & Taylor (2003). The lines as given by general relativity and with line widths that are larger than the corresponding uncertainties all intersect in a single point. right) Pulse profiles of the new DNSs PSR J0737−3039 (Burgay et al. 2003, top) and J1756−2256 (Faulkner et al., in prep., bottom). These systems promise to provide similar or even better tests than PSR B1913+16.

5.2   Tests using Double Neutron Stars

Even though in all metric theories matter and non-gravitational fields respond only to the space-time metric, it is possible that scalar or vector fields exist in addition to the metric. Damour & Esposito-Farèse developed a framework to study theories at a second post-Newtonian (2PN) level where gravity is mediated by a tensor field and one or more scalar field [9]. These theories are interesting since scalar partners to gravitons arise naturally in quantum gravity and unified theories. Damour & Esposito-Farèse show that it is possible to construct corresponding theories where deviations from general relativity are not visible in the weak field but only manifest themselves in a "spontaneous scalarization" if the strong field limit is approached. They conclude that current solar system tests and also upcoming satellite missions will not be able to replace the strong field tests provided by radio pulsars. Indeed, they use the DNSs, PSR B1534+12 and PSR B1913+16, together with PSR B0655+64 and solar system tests, to significantly constrain the parameters describing the coupling of matter to the scalar field [10]. A more classical approach using DNSs for tests of theories of gravity is made with the measurement of post-Keplerian (PK) parameters as observables.

Because of the strong gravitational fields, we expect DNSs to suffer large relativistic effects. In this case, we cannot necessarily assume that we understand the underlying physics, even though general relativity appears to describe the physics in the solar system to high precision. Therefore, a purely theory-independent approach like the PPN approximation is difficult to realize. Instead, one can only use an existing theory of gravity and check if the observations are

consistently described by the measured Keplerian and PK parameters. In each theory, the PK parameters should only be functions of the a priori unknown pulsar and companion mass, M_p and M_c, and the easily measurable Keplerian parameters. With the two masses as the only free parameters during the test, an observation of two PK parameters will already determine the masses uniquely in the framework of the given theory. The measurement of a third or more PK parameters then provides a consistency check. In general relativity, the five most important PK parameters are given by (e.g. [37]):

$$\dot{\omega} = 3T_\odot^{2/3} \left(\frac{P_b}{2\pi}\right)^{-5/3} \frac{1}{1-e^2} (M_p + M_c)^{2/3}, \tag{15}$$

$$\gamma = T_\odot^{2/3} \left(\frac{P_b}{2\pi}\right)^{1/3} e \frac{M_c(M_p + 2M_c)}{(M_p + M_c)^{4/3}} \tag{16}$$

$$\dot{P}_b = -\frac{192\pi}{5} T_\odot^{5/3} \left(\frac{P_b}{2\pi}\right)^{-5/3} \frac{\left(1 + \frac{73}{24}e^2 + \frac{37}{96}e^4\right)}{(1-e^2)^{7/2}} \frac{M_p M_c}{(M_p + M_c)^{1/3}}, \tag{17}$$

$$r = T_\odot M_c, \tag{18}$$

$$s = T_\odot^{-1/3} \left(\frac{P_b}{2\pi}\right)^{-2/3} x \frac{(M_p + 2M_c)^{2/3}}{M_c} \tag{19}$$

where P_b is the period and e the eccentricity of the binary orbit. The masses M_p and M_c of pulsar and companion, respectively, are expressed in solar masses ($M_\odot$). We define the constant $T_\odot = GM_\odot/c^3 = 4.925490947\mu s$ where G denotes the Newtonian constant of gravity and c the speed of light. The first PK parameter, $\dot{\omega}$, is the easiest to measure and describes the relativistic advance of periastron. According to Eqn. 15 it provides an immediate measurement of the total mass of the system, $(M_p + M_c)$. The parameter γ denotes the amplitude of delays in arrival times caused by the varying effects of the gravitational redshift and time dilation (second order Doppler) as the pulsar moves in its elliptical orbit at varying distances from the companion and with varying speeds. The decay of the orbit due to gravitational wave damping is expressed by the change in orbital period, $\dot{P}_b$. The other two parameters, r and s, are related to the Shapiro delay caused by the gravitational field of the companion. These parameters are only measurable, depending on timing precision, if the orbit is seen nearly edge-on.

Currently, only two DNSs have more than two PK parameters determined, the 59-ms pulsar B1913+16 and the 38-ms PSR B1534+12. For PSR B1913+16 with an eccentric ($e = 0.61$) 7.8-hr orbit, the PK parameters $\dot{\omega}$, γ and $\dot{P}_b$ are measured very precisely. Correcting the observed $\dot{P}_b$ value for the Shlovskii effect (see Section 4.1), the measured value is in excellent agreement with the prediction of general relativity for quadrupole emission. The dependencies of the PK parameters on the unknown pulsar and companion masses can be displayed in a M_p-M_c diagram where all lines meet in a single point (0.25% agreement, see Fig. 4). It demonstrates impressively that general relativity provides a self-consistent and accurate description of the system which can be described as orbiting point masses, i.e. the structure of the neutron stars does not influence their orbital

motion as expected from SEP. The precision of this test is limited by our knowledge of the Galactic gravitational potential and the corresponding correction to $\dot{P}_b$. The timing results for PSR B1913+16 provide us with the most precise measurements of neutron star masses ever, i.e. $M_p = (1.4408 \pm 0.0003) M_\odot$ and $M_c = (1.3873 \pm 0.0003) M_\odot$ [35]. It is worth pointing out that these values include the unknown Doppler factor.

The 10-hr orbit of the second DNS PSR B1534+14 ($e = 0.27$) is observed under fortunate circumstances, it is seen nearly edge-on. Thereby, in addition to the three PK parameters observed for PSR B1913+16, the Shapiro-delay parameters r and s can be measured, enabling non-radiative aspects of gravitational theories to be tested, as $\dot{P}_b$ is not necessarily needed. In fact, the observed value of $\dot{P}_b$ seems to be heavily influenced by Shlovskii-terms, so that the corresponding line fails to meet the others in a M_p-M_c diagram. However, assuming that general relativity is the correct theory of gravitation, the deviation from the predicted value and the measured proper motion, μ, can be used to compute the necessary correction and hence the distance to the pulsar, $d = 1.02 \pm 0.05$ kpc [31].

5.3   Tests Using Profile Structure Data

In addition to the use of pulsars as clocks, strong gravity effects can also be tested using pulse structure data, namely the effects of "geodetic precession" in the DNSs PSR B1913+16 and PSR B1534+14. In both cases, the pulsar spin axis appears to be misaligned with the orbital angular momentum vector. In such a case, general relativity predicts a relativistic spin-orbit coupling, analogous to spin-orbit coupling in atomic physics. The pulsar spin precesses about the total angular momentum, changing the relative orientation of the pulsar towards Earth. As a result, the angle between the pulsar spin axis and our line-of-sight changes with time, so that different portions of the emission beam are observed [11]. Consequently, changes in the measured pulse profile and its polarization are expected. In extreme cases, the precession may even move the beam out of our line-of-sight and the pulsar may disappear as predicted for PSR B1913+16 [18]. See the review by Kramer [19] for a detailed review.

5.4   Recent Discoveries

The tremendous success of recent surveys using the Parkes telescope (e.g. [24]) has lead not only to the discovery of more than 700 new pulsars, but also to some very exciting new binary systems. Until recently, only five DNSs were known. This situation has changed and now seven systems can be studied. PSR J0737-3039 was discovered in April 2003 [8] (see Fig. 4). The present observations already indicate that it is the most extreme relativistic binary system discovered so far: its short orbital period ($P_b = 2.4$ hrs) together with a remarkable high value of periastron advance ($\dot{\omega} = 16.88 \pm 0.09$ deg/yr, i.e. four times larger than for PSR B1913+16!) and the short coalescing time (~ 85 Myr) make this system the most beautiful laboratory for testing general relativity found so far.

Moreover, with a geodetic precession period of only 70 yr future studies should reveal interesting and exciting results. Even more recently, another DNS was discovered in the Parkes Multibeam (PM) Survey, PSR J1756−2256 (Faulkner et al., in prep., Fig. 4). This system shows similarities with PSR B1913+16 as its orbital period is somewhat less than 8 hours although its eccentricity is smaller ($e = 0.18$). The recent discoveries benefit from larger available computing power which enables so-called "acceleration searches" for fast orbiting binary pulsars. For instance, another fast binary discovered in the PM Survey in February 2003 using an acceleration code is PSR J1743−3924 (Lyne, priv. communication). This 172.44-ms pulsar is in an almost circular 4.6-hr orbit and hence only the second non-recycled pulsar in such a short orbit. The other such pulsar is PSR J1141−6545 which is a 393-ms PM pulsar in 4.5-hr orbit [15]. Both pulsars appear to have a white dwarf companion, but while PSR J1141−6545's companion is heavy ($M_c \sim 1M_\odot$), the new pulsar's companion is probably much lighter ($M_c \geq 0.08M_\odot$). Even if the companion is not a neutron star, strong-field effects can nevertheless be observed (e.g. [15]), but tests are limited due to the lower timing precision of the slower rotating pulsars. The hunts for DNSs will continue.

6   Conclusions & Outlook

Millisecond pulsars find a wide range of applications, in particular for precise tests of theories of gravity. After the discovery of pulsars thereby marked the beginning of a new era in fundamental physics, pulsars discovered and observed with the future Square-Kilometer-Array (SKA) will further transform our understanding of gravitational physics. The SKA's sensitivity will discover the majority of pulsars in the Galaxy, almost certainly providing the discovery of the first pulsar-black hole system. For tests of general relativity such a system would have with a discriminating power that surpasses all its present and foreseeable competitors [10]. Moreover, the pulsars would act as arms of a huge gravitational wave detector enabling the study of a possible gravitational wave background in a frequency range that is inaccessible to LIGO or even LISA. Clearly, the SKA will provide yet another leap in our understanding and application of pulsars.

References

1. Alpar, M. A., Cheng, A. F., Ruderman, M. A. & Shaham, J., Nature, **300**, 728 (1982)
2. Arzoumanian, Z., PhD thesis, Princeton University (1995)
3. Backer, D. C. & Hellings, R. W., Ann. Rev. Astr. Ap., **24**, 537 (1986)
4. Backer, D. C., Kulkarni, S. R., Heiles, C., Davis, M. M. & Goss, W. M., Nature, **300**, 615 (1982)
5. Bell, J. F. & Damour, T., Class. Quantum Grav., **13**, 3121 (1996)
6. Bell, J. F., ApJ, **462**, 287 (1996)
7. Bignami, G. F., Caraveo, P. A., Luca, A. D. & Mereghetti, S., Nature, **423**, 725 (2003)
8. Burgay, M., D'Amico, N., Possenti, et al., Nature, in press (2003)

9. Damour, T. & Esposito-Farèse, G., Phys. Rev. D, **53**, 5541–5578 (1996)
10. Damour, T. & Esposito-Farèse, G., Phys. Rev. D, **58**, 042001–1 (1998)
11. Damour, T. & Ruffini, R., Academie des Sciences Paris Comptes Rendus Ser. Scie. Math., **279**, 971 (1974).
12. Damour, T. & Schäfer, G., Phys. Rev. Lett., **66**, 2549 (1991)
13. Damour, T., Gibbons, G. W. & Taylor, J. H., Phys. Rev. Lett., **61**, 1151 (1988)
14. Hankins, T. H., Kern, J. S., Weatherall, J. C. & Eilek, J. A., Nature, **422**, 141 (2003)
15. Kaspi, V. M., Lyne, A. G., Manchester, R. N., et al., ApJ, **543**, 321 (2000)
16. Kaspi, V. M., Taylor, J. H. & Ryba, M., ApJ, **428**, 713 (1994)
17. Kramer, M., Xilouris, K. M., Jessner, A., et al., A&A, A&A, **322**, 846 (1997)
18. Kramer, M., ApJ, **509**, 856 (1998)
19. Kramer, M., In: *The Ninth Marcel Grossmann Meeting*, eds V.G. Gurzadyan, R.T. Jantzen & R. Ruffini (World Scientific, Singapore 2002) pp. 219
20. Kramer, M., Lyne, A. G., Hobbs, G., et al., ApJ, **593**, L31 (2003)
21. Lange, C., Camilo, F., Wex, N., et al., MNRAS, **326**, 274 (2001)
22. Lorimer, D. R., Living Rev. Relativity, **4**. 5. [Online article]: cited on 1 Oct 2003, http://www.livingreviews.org/lrr-2001-5 (2001)
23. Lyne, A. G., Pritchard, R. S. & Smith, F. G., MNRAS, **265**, 1003 (1993)
24. Manchester, R. N., Lyne, A. G., Camilo, F., et al., MNRAS, **328**, 17 (2001)
25. McLaughlin, M. A., Stairs, I. H., Kaspi, V. M., et al., ApJ, **591**, L135 (2003)
26. Nordtvedt, K., Phys. Rev., **170**, 1186 (1968)
27. Oppenheimer, J. R. & Volkoff, G., Phys. Rev., **55**, 374 (1939)
28. Phinney, E. S., Philos. Trans. Roy. Soc. London A, **341**, 39 (1992)
29. Shapiro, I. I., Phys. Rev. Lett., **13**, 789 (1964)
30. Stairs, I. H., Living Rev. Relativity, **6**. 5. [Online article]: cited on 1 Oct 2003, http://www.livingreviews.org/lrr-2003-5 (2003)
31. Stairs, I. H., Thorsett, S. E., Taylor, J. H. & Wolszczan, A., ApJ, **581**, 501 (2002)
32. Standish, E. M., A&A, **114**, 297 (1982)
33. Thorsett, S. E., Phys. Rev. Lett., **77**, 1432 (1996)
34. Thorsett, S. E. & Chakrabarty, D., ApJ, **512**, 288 (1999)
35. Weisberg, J. M. & Taylor, J. H., In: *Radio Pulsars*, eds M. Bailes, D.J. Nice & S.E. Thorsett, ASP Conf. Series Vol. 302 (PASP, San Francisco 2003), pp. 93
36. Wex, N., In: *Pulsar Astronomy - 2000 and Beyond, IAU Colloquium 177*, eds M. Kramer, N. Wex & R. Wielebinski, R., ASP Conf. Series Vol. 202 (PASP, San Francisco 2000), pp. 113
37. Wex, N., In: *Gyros, Clocks, Interferometers...: Testing Relativistic Gravity in Space*, eds Lämmerzahl, C. & Everitt, C. W. F. Hehl, F. W., (Springer, 2001)
38. Will, C. M., ApJ, **393**, L59 (1992)
39. Will, C. M., *Theory and Experiment in Gravitational Physics*, (Cambridge University Press, Cambridge 1993)
40. Will, C. M., Living Rev. Relativity, **4**. 4. [Online article]: cited on 1 Oct 2003, http://www.livingreviews.org/lrr-2001-4 (2001)
41. Young, M. D., Manchester, R. N. & Johnston, S., Nature, **400**, 848 (1999)
42. Zavlin, V. E., Pavlov, G. G., A&A, **329**, 583 (1998)